metals

MDPI

Article

Study of Adsorption of Hydrogen on Al, Cu, Mg, Ti Surfaces in Al Alloy Melt via First Principles Calculation

Yu Liu [1,2,*], Yuanchun Huang [1,2,3,*], Zhengbing Xiao [1,2,3] and Xianwei Reng [1,2]

1 Research Institute of Light Alloy, Central South University, Changsha 410083, China; xiaozb@csu.edu.cn (Z.X.); renxianweichina@126.com (X.R.)
2 Nouferrous Metal Oriented Advanced Structural Materials and Manufacturing Cooperative Innovation Center, Central South University, Changsha 410083, China
3 College of Mechanical and Electrical Engineering, Central South University, Changsha 410083, China
* Correspondence: csuliuyu@csu.edu.cn (Y.L.); science@csu.edu.cn (Y.H.); Tel.: +86-152-7312-0641 (Y.H.); Fax: +86-73-188877315 (Y.H.)

Academic Editor: Hugo F. Lopez
Received: 4 November 2016; Accepted: 13 December 2016; Published: 11 January 2017

Abstract: Adsorption of hydrogen on Al(111), Cu(111), Mg(0001), and Ti(0001) surfaces have been investigated by means of first principles calculation. The calculation of surface energy indicates that Mg(0001) is the most stable surface, while Ti(0001) is the most unstable surface among all the four calculated surfaces. The obtained adsorption energy shows that the interaction between Al and H atoms should be energetically unfavorable, and the adsorption of hydrogen on Mg(0001) surface was found to be energetically preferred. Besides, the stability of hydrogen adsorption on studied surfaces increased in the order of Al(111), Ti(0001), Cu(111), Mg(0001). Calculation results also reveal that hydrogen adsorption on fcc and hcp sites are energetically stable compared with top and bridge sites for Ti(0001), Cu(111), and Mg(0001), while hydrogen adsorbing at the top site of Al(111) is the most unstable state compared with other sites. The calculated results agreed well with results from experiments and values in other calculations.

Keywords: surface energy; hydrogen adsorption; stability; first principles calculation

1. Introduction

Aluminum alloy has been widely used in the aeronautics industry, space industry, nuclear industry, and military industry for its low density, high strength, and anti-corrosive ability [1–3]. Numerous efforts have been devoted to improving the quality of aluminum alloy products, so as to meet the increasing demands for high performance from composition and processing technology.

It is widely recognized that the first step to ensure the properties of an aluminum component is a high-quality ingot, since it plays a key role in determining the microstructure evolution in subsequent processing steps. In order to prepare such an ingot, the purification process of liquid aluminum alloys prior to casting has a crucial importance. The purpose of purification is to remove impurities from molten metals, which may be in the form of gases, inclusions, or dissolved metals, which may lead to casting defects.

Porosity—a frequent casting defect—has proven to be a challenge for its formation and evolution. At present, it is believed that one of the main reasons for porosity formation in aluminum alloys is attributable to hydrogen evolution. In fact, hydrogen is supposed to be the only gas dissolved in aluminum melt [4,5]. When the hydrogen content reaches a critical value in the liquid metal, molecular hydrogen pores form and may grow depending on the local hydrogen concentration levels and the diffusion rate [6]. This kind of gas porosity is normally observed only as small distributed pores, which

are also termed microporosity. The formed microporosities have detrimental effects on both the service and processing properties of metals. Hence, the removal of the hydrogen from the aluminum melt is crucial for the production of high-quality castings.

Several approaches have been developed for degassing in the last several decades; for example, re-melting degassing [7], vacuum degassing [8,9], ultrasonic degassing [10,11], and spray degassing [12,13], as well as rotary impeller degassing with nitrogen, argon, or a mixture of the inert gases and chlorine as a purge gas [14–16]. Nevertheless, the research on technology and equipment of high-efficiency degassing depends on reliable physical property data and parameters of degassing mechanisms, which are still incompletely understood.

In terms of hydrogen removal, it is necessary to have a good understanding of the interaction between hydrogen and the components of the aluminum melt (such as alloying elements and inclusions) for an efficient hydrogen removal. Anyalebechi analyzed the effects of alloying elements on the solubility of hydrogen in liquid aluminum via Wagner's interaction parameter [17]. However, investigation of the interaction between hydrogen and the component of the aluminum melt is limited to experimental equipment and technology. Recently, first-principles calculations based on density functional theory have been widely used in interfacial research for their high reliability and accuracy.

To our knowledge, few systematic and theoretical studies regarding the interaction between hydrogen and alloying elements in molten aluminum have been reported. Therefore, the aim of the present work is to study the adsorption of hydrogen on the alloying element surfaces of Cu, Mg, and Ti from first-principles calculations, and the matrix element is also calculated for comparison.

2. Computational Methods

The first-principles calculation was carried out by means of the Cambridge Sequential Total Energy Package (CASTEP, Accelrys, San Diego, CA, USA), and the calculation was conducted in a plane-wave basis using the projector-augmented wave (PAW) method [18]. The interaction between ions and electrons was described using the ultrasoft pseudopotentials introduced by Vanderbilt and provided by Kresse and Hafner [19]. The exchange correlation functional was described by general gradient approximation (GGA) of Perdew-Burke-Ernzerhof (PBE), convergence tolerance of total energy per atom is 2×10^{-6} eV, and the Brodygen-Fletcher-Gplldfarb-Shanno (BFGS) [19,20] method was used for optimization.

The present studies of surface energy and H adsorption are focused on low-index surfaces as typical examples owing to their close-packed nature and lower energy state; i.e., (0001) of Mg and Ti, (111) of Al and Cu. Accordingly, a $2 \times 2 \times 1$ unit cell was selected for (111) of Cu, (0001) of Mg and Ti, and 1×1 unit cell for Al(111).

After the test, a seven-layer slab of Al, Mg, and Ti, with a vacuum thickness between any two successive metal slabs of 2.7, 2.1, and 1.75 nm, respectively, and a six-layer slab of Cu with a vacuum thickness of 2.7 nm were used for the calculation of surface energy and adsorption energy.

The influence of different k-point sampling and plane-wave cutoff energy were performed in a series of test calculations, and this led to the calculations being performed with $17 \times 17 \times 1$ and $21 \times 21 \times 1$ k-point sampling and a cutoff energy of 450 for Al(111) and Cu(111), and 480 eV for Mg(0001) and Ti(0001), respectively. The above parameters were determined to be high enough to ensure accuracy.

For the adsorption of H atoms, both of FCC and HCP structures have four adsorption positions. Accordingly, Figure 1 shows the schematic illustrations of various adsorption positions of H; i.e., the top (A), fcc (B), bridge (C), and hcp (D) sites of FCC (111) or HCP (0001) surface. For H adsorption on each slab, the atoms in the top two layers and the adsorbate were allowed to relax, while the atoms in other layers were fixed at the bulk truncated positions.

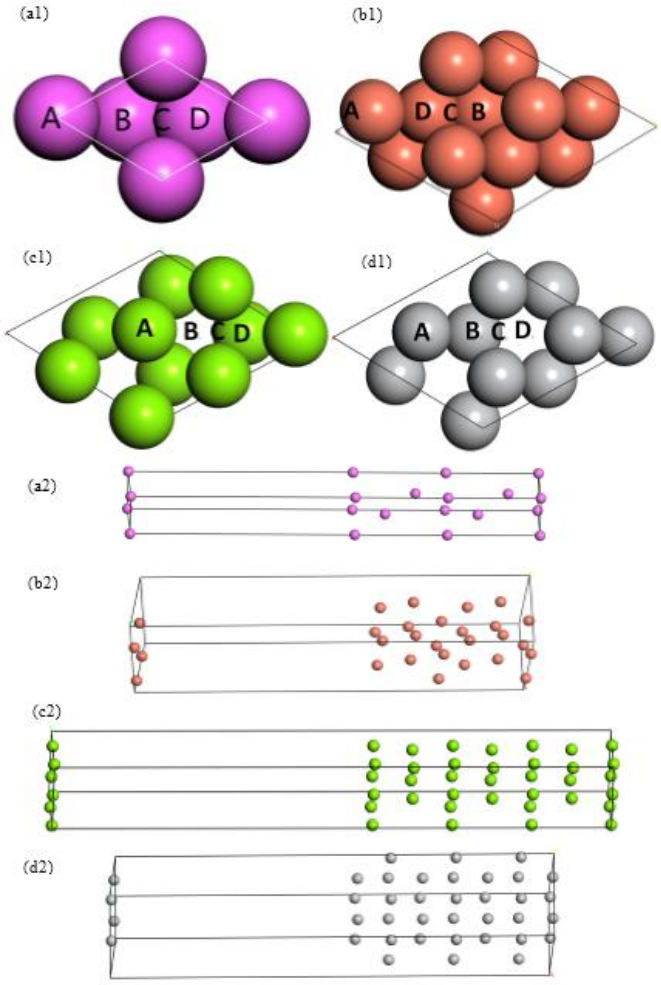

Figure 1. Schematic illustration of adsorption sites of H on (111) surface of (**a1**) Al and (**b1**) Cu; (0001) surface of (**c1**) Mg and (**d1**) Ti; together with the side structure of model surface of (**a2**) Al(111), (**b2**) Cu(111), (**c2**) Mg(0001), and (**d2**) Ti(0001). A—Top site, B—Fcc site, C—Bridge site, D—Hcp site.

3. Results and Discussion

3.1. Surface Energy and Work Function of Al, Cu, Mg, and Ti

Before surface calculation, geometry optimization was conducted on all the bulk structures, and the obtained lattice constants are listed in Table 1. It could be seen that the present lattice constants (Al: a = 4.021 Å; Cu: a = 3.641 Å; Mg: a = 3.192 Å, c = 5.206 Å; Ti: a = 2.896 Å, c = 4.626 Å) are consistent with corresponding experimental values in the literature and values in other calculations. Hence, the computation parameters and model setting above can provide reliable description for the calculation system, and the obtained bulks are used in the following interface modeling and computations of surface energy and adsorption energy.

Table 1. Lattice constants of Al, Cu, Mg, and Ti.

Elements	Lattice Constants (Å)		
	This Work	**Experiments**	**Other Calculation**
Al	a = 4.021	a = 4.05 [20]	a = 3.982 [21]
Cu	a = 3.641	a = 3.61 [22]	a = 3.638 [23]
Mg	a = 3.192, c = 5.206	a = 3.21, c = 5.213 [24]	a = 3.19, c = 5.17 [25]
Ti	a = 2.896, c = 4.626	a = 2.904, c = 4.680 [26]	a = 2.864, c = 4.537 [21]

Surface modeling of FCC and HCP structures were performed based on the obtained bulk structures, and the calculation of surface energy and work function of Al(111), Cu(111), Mg(0001), and Ti(0001) surfaces were performed by means of the following formulas [27]:

$$\gamma = 1/2A \times (E_{\text{slab}} - E_{\text{bulk}}) \quad (1)$$

$$\Phi = V_{\text{vac}} - E_f \quad (2)$$

where γ is surface energy, A is the surface area, E_{slab} is the total energy of the slab, E_{bulk} is the total energy of the corresponding bulk, and the factor $1/2$ in Equation (1) is owing to two equivalent surfaces in the slab, Φ is the work function, V_{vac} is the vacuum level in the vacuum region, and E_f stands for the Fermi energy of the slab.

The surface energy of Al(111), Cu(111), Mg(0001), and Ti(0001) were calculated via Equation (1), the computation results are listed in Table 2, and values from other sources are also presented for comparison. One can obviously deduce from Table 2 that the surface energy of Ti(0001) is the highest, which was calculated to be 2.034 J/m^2; the surface energy of Mg(0001) was lowest, which was calculated to be 0.716 J/m^2; and the surface energy of Al(111) and Cu(111) was located between the above two values. All of the calculation results agreed quite well with values from other sources, which again validates the computation details.

Surface energy is one of the basic quantities in surface physics, and is defined as the surface excess free energy per unit area of a particular crystal facet; that is, the energy required to cut a crystal into two parts or two surfaces. It is important in surface faceting, roughening, and crystal growth phenomena, and may be used to estimate surface segregation in binary alloys. On the other hand, the surface energy can be a measure of the stability of the surface—a lower surface energy indicates a more stable surface; that is to say, Mg(0001) is the most stable surface, and Al(111) follows, while Ti(0001) is the most unstable surface among all the four calculated surfaces.

Table 2. Surface energy of Al(111), Cu(111), Mg(0001), and Ti(0001).

Surface	Surface Energy (J/m^2)		
	This Work	Experiments	Other Calculation
Al(111)	0.864	1.14 [28]	0.988 [21]
Cu(111)	1.793	1.825 [28]	1.94 [29]
Mg(0001)	0.716	0.785 [28]	0.641 [30]
Ti(0001)	2.034	1.98 [31]	2.235 [21]

The work function of Al(111), Cu(111), Mg(0001), and Ti(0001) were calculated to be 4.26, 4.98, 3.80, and 4.58 eV, respectively, according to Equation (2), as listed in Table 3. The derived work functions are consistent with values in literature, and the maximum deviation of work function is 0.13 eV for Ti(0001).

Table 3. Work function of Al(111), Cu(111), Mg(0001), and Ti(0001).

Surfaces	Work Function (eV)		
	This Work	Experiments	Other Calculation
Al(111)	4.26	4.24 [32]	4.22 [21]
Cu(111)	4.98	4.94 [33]	5.1 [29]
Mg(0001)	3.80	3.86 [34]	3.76 [35]
Ti(0001)	4.58	4.45 [36]	4.67 [21]

The work function is a property of the surface of the material which is defined as the minimum thermodynamic energy needed to remove an electron from a solid to a point in the vacuum immediately outside the solid surface. In other words, it reflects the difficulty of losing an electron for a given

surface, and the ability to lose electrons decreases with increasing work function. The work function of Cu(111) is the highest, which shows that it is the most difficult to lose electrons. Accordingly, the ability of the above surfaces to lose electrons is ranked as Mg(0001), Al(111), Ti(0001), Cu(111), in decreasing order.

3.2. Electronic Structures of Slabs

It is of great importance to investigate the electronics structures of Al(111), Cu(111), Mg(0001), and Ti(0001) surfaces. Figure 2 shows the comparison of total density of states (DOS) of Al, Cu, Mg, and Ti atoms in the bulk and surface. It can be seen that for all atoms—Al, Cu, Mg, and Ti—the bandwidths of DOS of the surface atoms are smaller than those of the bulk atom. Another feature that can be deduced from Figure 2 is that the DOSs of analyzed atoms in the surface have higher values around the Fermi level than those atoms in bulk. It is easy to derive the conclusion that some changes of electronic structures have occurred during surface formation for Al(111), Cu(111), Mg(0001), and Ti(0001).

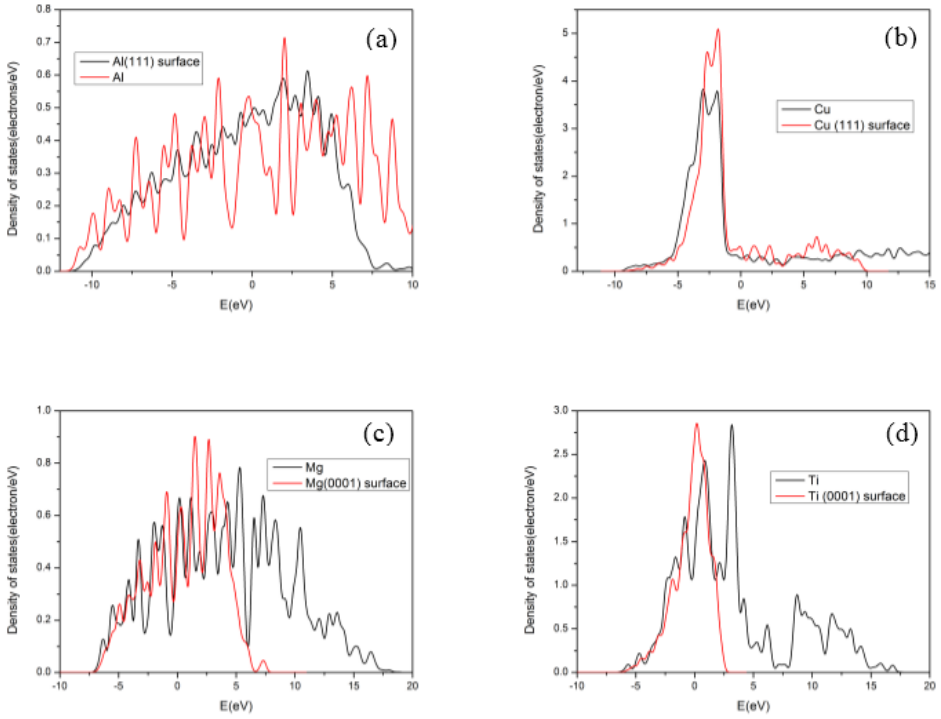

Figure 2. Density of states (DOS) of (**a**) Al; (**b**) Cu; (**c**) Mg; and (**d**) Ti in the bulk and surface.

3.3. H Adsorption on Al(111), Cu(111), Mg(0001), and Ti(0001) Surfaces

The adsorption energy (E_{ads}) of H on Al(111), Cu(111), Mg(0001), and Ti(0001) surfaces are derived according to the following formula:

$$E_{ads} = E_{H\text{-}slab} - E_{slab} - E_{H_2}/2 \quad (3)$$

where $E_{H\text{-}slab}$ and E_{slab} are total energies of the slab with and without H adsorption, respectively, and E_{H2} is the total energy of a H_2 molecule.

After a series of calculations, the adsorption energy of H is obtained for various adsorption sites of Al(111), Cu(111), Mg(0001), and Ti(0001) surfaces as Figure 1 shows, and the results are summarized in Table 4. Though experimentally-derived values of the adsorption energy of hydrogen atoms on element surfaces are still missing, we list values from references for comparison in the present paper to verify the reliability of this study.

It should be noted that during the calculation of H adsorption on the bridge site of Al(111) and Ti(0001), the adsorbates will move to fcc site and hcp site, respectively, after relaxation calculation, which reveals that hydrogen adsorption at bridge sites of Al(111) and Ti(0001) is energetically unstable.

Table 4. Adsorption energy (E_{ads}) of hydrogen on various adsorption sites of Al(111), Cu(111), Mg(0001), and Ti(0001) surfaces.

Surface	Sites	E_{ads} (eV)	
		This Work	**Other Calculation**
Al(111)	Top	0.235	0.226 [a]
	Fcc	0.081	0.069 [a]
	Hcp	0.132	0.122 [a]
Cu(111)	Top	−1.667	−1.83 [b]
	Fcc	−2.385	−2.37 [b]
	Hcp	−2.353	−2.36 [b]
	Bridge	−2.178	−2.22 [b]
Mg(0001)	Top	−1.21	−1.04 [c]
	Fcc	−2.546	−2.56 [c]
	Hcp	−2.471	−2.52 [c]
	Bridge	−1.90	−1.89 [c]
Ti(0001)	Top	0.610	0.400 [a]
	Fcc	−1.486	−1.342 [a]
	Hcp	−1.502	−1.396 [a]

[a] Reference [21]; [b] Reference [37]; [c] Reference [25].

Several highlights could be deduced from Table 4. Firstly, our calculation results agree quite well with values from other sources. Secondly, one sees clearly from Table 4 that for Al(111) surface, the E_{ads} values of hydrogen adsorbed on all sites are positive, suggesting that the interaction between Al and H atoms should be mainly repulsive and energetically unfavorable. Thirdly, it seems more likely that the adsorption of hydrogen on the Mg(0001) surface was found to be energetically preferred, due to the E_{ads} of −2.546, −2.471, and −1.90 eV for hydrogen adsorbed on fcc, hcp, and bridge sites of Mg(0001), respectively. As a whole, the stability of hydrogen adsorption on the studied surfaces increased in the order of Al(111), Ti(0001), Cu(111), Mg(0001). The stability of hydrogen on fcc and hcp sites is energetically stable compared with top and bridge sites for Ti(0001), Cu(111), and Mg(0001). Hydrogen adsorbing at the top site of Al(111) is the most unstable state compared with other site of Al(111).

On the other hand, we also calculate the heat of formation of hydrogen adsorption (ΔH_e) to compare the stability of hydrogen on Al(111), Cu(111), Mg(0001), and Ti(0001) surfaces. Accordingly, ΔH_f is calculated by means of the following formula:

$$\Delta H_f = \frac{1}{N}(E_{\text{H-slab}} - E_{\text{slab}} - E_{H_2}/2) \quad (4)$$

where N is the total number of atoms in the system, $E_{\text{H-slab}}$, E_{slab}, and E_{H2} have the same meaning as mentioned above. The calculated ΔH_f are presented in Table 5.

Table 5. Heat of formation (ΔH_f) of hydrogen on various adsorption sites of Al(111), Cu(111), Mg(0001), and Ti(0001) surfaces.

Sites		Top	Fcc	Hcp	Bridge
ΔH_f (kJ/mol)	Al_8H	5.04	1.74	2.83	
	$Cu_{24}H$	−12.86	−18.40	−18.15	−16.80
	$Mg_{29}H$	−7.78	−16.37	−15.89	−12.22
	$Ti_{28}H$	4.06	−9.88	−9.99	

It can be seen that the ΔH_f of hydrogen adsorbed on Al(111) are all positive, while in other systems, only hydrogen adsorbed on the top site of Ti(0001) is positive. ΔH_f of hydrogen adsorbed on Cu(111) are much closer to each other. In terms of $Mg_{29}H$, the lowest and highest ΔH_f occur in the Fcc site and top sites, respectively, and the ΔH_f of hydrogen adsorbed on Fcc and Hcp site of Ti(0001) are almost equal. A lower heat of formation suggests a stronger interaction between H and the surface; that is to say, the interaction between H and the studied surfaces decreased in the order Al(111), Ti(0001), Cu(111), Mg(0001). The conclusion deduced from ΔH_f agrees well with what is indicated by E_{ads}.

Accordingly, it is more likely for hydrogen atoms to adsorb on Cu and Mg surfaces than Al and Ti. On the other hand, we can conclude that relatively more energy is required to remove a hydrogen atom from Mg and Cu surfaces, and less energy to remove a hydrogen atom from Al surfaces. Besides, for the studied elements Al, Cu, Mg, and Ti, the hydrogen solubility of molten aluminum suffers most from Cu and Mg, in short range atomic group, and Ti follows. Based on the obtained calculation results, theoretical guidance can be provided for hydrogen removal from aluminum melt.

4. Summary and Conclusions

The adsorption of hydrogen on Al(111), Cu(111), Mg(0001), and Ti(0001) surfaces has been investigated by means of first principles calculation, and several remarks could be drawn from the computation results. Firstly, Mg(0001) is the most stable surface, while Ti(0001) is the most unstable surface among all the four calculated surfaces, and the ability of the above surfaces to lose electrons is ranked as Mg(0001), Al(111), Ti(0001), and Cu(111) in decreasing order. Secondly, the interaction between Al and H atoms should be energetically unfavorable, and the adsorption of hydrogen on the Mg(0001) surface were found to be energetically preferred, due to the E_{ads} of -2.546, -2.471, and -1.90 eV for hydrogen adsorbed on fcc, hcp, and bridge sites of Mg(0001), respectively. Thirdly, the stability of hydrogen adsorption on the studied surfaces increased in the order Al(111), Ti(0001), Cu(111), Mg(0001). Fourthly, hydrogen adsorption on fcc and hcp sites are energetically stable compared with top and bridge sites for Ti(0001), Cu(111), and Mg(0001). Hydrogen adsorbing at the top site of Al(111) is the most unstable state compared with other sites. Finally, the calculated results agree well with results from experiments and values in other calculations.

Acknowledgments: The authors are grateful for the financial supported by the Fundamental Research Funds for the Central Universities of Central South University(2015zzts042), the National Basic Research Program of China (2015CB057305).

Author Contributions: Yu Liu and Yuanchun Huang conceived and designed the calculations; Yu Liu performed the calculations; Yu Liu and Yuanchun Huang analyzed the data; Zhengbing Xiao and Xianwei Ren contributed analysis tools; Yu Liu wrote the paper.

Conflicts of Interest: The authors declare no conflict of interest.

References

1. Wanhill, R.J.H.; Bray, G.H. Chapter 2—Aerostructural Design and Its Application to Aluminum-Lithium Alloys. *Alum. Lithium Alloy.* **2014**, *14*, 27–58.
2. Li, Y.-P. Application and Prospect of Aluminum Alloys Automobile industry. *Alum. Fabr.* **2007**, *173*, 23–24.
3. Shi, Q.; Xiong, W. Application and Development of Aluminium Alloys in Automobile Industry. *New Technol. New Process* **2006**, *12*, 55–58.
4. Poirier, D.R.; Yeum, K.; Maples, A.L. A thermodynamic prediction for microporosity formation in aluminum-rich Al-Cu alloys. *Metall. Trans. A* **1987**, *18*, 1979–1987. [CrossRef]
5. Han, Q.; Viswanathan, S. Hydrogen evolution during directional solidification and its effect on porosity formation in aluminum alloys. *Metall. Mater. Trans. A* **2002**, *33*, 2067–2072. [CrossRef]
6. Felberbaum, M.; Désy, E.L.; Weber, L.; Rappaz, M. Effective hydrogen diffusion coefficient for solidifying aluminium alloys. *Acta Mater.* **2011**, *59*, 2302–2308. [CrossRef]
7. Zhao, L.; Pan, Y.; Liao, H.; Wang, Q. Degassing of aluminum alloys during re-melting. *Mater. Lett.* **2012**, *66*, 328–331. [CrossRef]

8. Xu, H.; Meek, T.T.; Han, Q. Effects of ultrasonic field and vacuum on degassing of molten aluminum alloy. *Mater. Lett.* **2007**, *61*, 1246–1250. [CrossRef]
9. Zhu, X.; Jiang, D.; Tan, S. Improvement in the strength of reticulated porous ceramics by vacuum degassing. *Mater. Lett.* **2001**, *51*, 363–367. [CrossRef]
10. Éskin, G.I. Prospects of ultrasonic (cavitational) treatment of the melt in the manufacture of aluminum alloy products. *Metallurgist* **1998**, *42*, 284–291. [CrossRef]
11. Eskin, G.I. Principles of Ultrasonic Treatment: Application for Light Alloys Melts. *Adv. Perform. Mater.* **1997**, *4*, 223–232. [CrossRef]
12. Wu, R.; Shu, D.; Sun, B.; Wang, J.; Li, F.; Chen, H.; Lu, Y. Theoretical analysis and experimental study of spray degassing method. *Mater. Sci. Eng. A* **2005**, *408*, 19–25. [CrossRef]
13. Wu, R.; Qu, Z.; Sun, B.; Shu, D. Effects of spray degassing parameters on hydrogen content and properties of commercial purity aluminum. *Mater. Sci. Eng. A* **2007**, *456*, 386–390. [CrossRef]
14. Warke, V.S.; Tryggvason, G.; Makhlouf, M.M. Mathematical modeling and computer simulation of molten metal cleansing by the rotating impeller degasser: Part I. Fluid flow. *J. Mater. Process. Technol.* **2005**, *168*, 112–118. [CrossRef]
15. Warke, V.S.; Shankar, S.; Makhlouf, M.M. Mathematical modeling and computer simulation of molten aluminum cleansing by the rotating impeller degasser: Part II. Removal of hydrogen gas and solid particles. *J. Mater. Process. Technol.* **2005**, *168*, 119–126. [CrossRef]
16. Wang, L.; Guo, E.; Huang, Y.; Lu, B. Rotary impeller refinement of 7075Al alloy. *Rare Met.* **2009**, *28*, 309–312. [CrossRef]
17. Anyalebechi, P.N. Analysis of the effects of alloying elements on hydrogen solubility in liquid aluminum alloys. *Scri. Metall. Mater.* **1995**, *33*, 1209–1216. [CrossRef]
18. Kresse, G.; Joubert, D. From Ultrasoft Pseudopotentials to the Projector Augmented-Wave Method. *Phys. Rev. B Condens. Matter* **1999**, *59*, 1758–1775. [CrossRef]
19. Kresse, G.; Hafner, J. Norm-conserving and ultrasoft pseudopotentials for first-row and transition elements. *J. Phys. Condens. Matter* **1994**, *6*, 8245. [CrossRef]
20. Zope, R.R.; Mishin, Y. Interatomic potentials for atomistic simulations of the Ti-Al system. *Phys. Rev. B* **2003**, *68*, 024102. [CrossRef]
21. Wang, J.W.; Gong, H.R. Adsorption and diffusion of hydrogen on Ti, Al, and TiAl surfaces. *Int. J. Hydrog. Energy* **2014**, *39*, 6068–6075. [CrossRef]
22. Straumanis, M.E.; Yu, L.S. Lattice parameters, densities, expansion coefficients and perfection of structure of Cu and of Cu—In α phase. *Acta Crystallogr.* **1969**, *25*, 676–682. [CrossRef]
23. Ganne, J.P.; Lebourgeois, R.; Paté, M.; Dubreuil, D; Pinier, L.; Pascard, H. The electromagnetic properties of Cu-substituted garnets with low sintering temperature. *J. Eur. Ceram. Soc.* **2007**, *27*, 2771–2777. [CrossRef]
24. Kittel, C. *Introduction to Solid State Physics*, 8th ed.; Addison-Wiley: New York, NY, USA, 2005.
25. Wu, G.-X.; Zhang, J.Y.; Wu, Y.-Q.; Li, Q.; Chou, K.; Bao, X.H. First-Principle Calculations of the Adsorption, Dissociation and Diffusion of Hydrogen on the Mg(0001) Surface. *Acta Phys. Chim. Sin.* **2008**, *24*, 55–60. [CrossRef]
26. Martin, A.S.; Manchester, F.D. The H-Ti (Hydrogen-Titanium) system. *Bull. Alloy Phase Diagr.* **1987**, *8*, 30–42. [CrossRef]
27. Halas, S.; Durakiewicz, T.; Joyce, J.J. Surface energy calculation—Metals with 1 and 2 delocalized electrons per atom. *Chem. Phys.* **2002**, *278*, 111–117. [CrossRef]
28. Tyson, W.R.; Miller, W.A. Surface free energies of solid metals: Estimation from liquid surface tension measurements. *Surf. Sci.* **1977**, *62*, 267–276. [CrossRef]
29. Polatoglou, H.M.; Methfessel, M.; Scheffler, M. Vacancy-formation energies at the (111) surface and in bulk Al, Cu, Ag, and Rh. *Phys. Rev. B* **1993**, *48*, 1877–1883. [CrossRef]
30. Wright, A.F.; Feibelman, P.J.; Atlas, S.R. First-principles calculation of the Mg(0001) surface relaxation. *Surf. Sci.* **1994**, *302*, 215–222. [CrossRef]
31. Murr, L.E. *Interfacial Phenomena in Metals and Alloys*; Addison-Wesley: Upper Saddle River, NJ, USA, 1974.
32. Michaelson, H.B. The work function of the elements and its periodicity. *J. Appl. Phys.* **1977**, *48*, 4729–4733. [CrossRef]
33. DeBoer, F.R.; Boom, R.; Mattens, W.C.M.; Miedema, A.R.; Niessen, A.K. *Cohesion in Metals*; HoIIand, N., Ed.; North Holland: Amsterdam, The Netherlands, 1988.

34. Skriver, H.L.; Rosengaard, N.M. Surface energy and work function of elemental metals. *Phys. Rev. B* **1992**, *46*, 7157–7168. [CrossRef]
35. Ji, D.-P.; Zhu, Q.; Wang, S.-Q. Detailed first-principles studies on surface energy and work function of hexagonal metals. *Surf. Sci.* **2016**, *651*, 137–146. [CrossRef]
36. Krumbein, A.D.; Malamud, H. Measurement of the effect of chlorine treatment on the work function of titanium and zirconium. *J. Appl. Phys.* **1954**, *25*, 591–592.
37. Strömquist, J.; Bengtsson, L.; Persson, M.; Hammer, B. The dynamics of H absorption in and adsorption on Cu(111). *Surf. Sci.* **1998**, *397*, 382–394. [CrossRef]

© 2017 by the authors; licensee MDPI, Basel, Switzerland. This article is an open access article distributed under the terms and conditions of the Creative Commons Attribution (CC-BY) license (http://creativecommons.org/licenses/by/4.0/).